Proceedings of 12th Cambridge Workshop on Cool Stars, Stellar Systems, & The Sun, 2003 University of Colorado.

Mass Loss Rates for Solar-like Stars Measured from Lyα Absorption

Brian E. Wood[1], Hans-Reinhard Müller[2], Gary P. Zank[2], Jeffrey L. Linsky[1]

Abstract.

We present a number of mass loss rate measurements for solar-like stars with coronal winds, computed using a Lyα absorption technique. The collision between the solar wind and the interstellar wind seen by the Sun defines the large scale structure of our heliosphere. Similar structures, "astrospheres," exist around other solar-like stars. The deceleration of the interstellar wind at the solar or stellar bow shock heats the interstellar material. Heated neutral hydrogen in the outer astrosphere (and/or heliosphere) produces a broad Lyα absorption profile that is often detectable in high resolution Hubble Space Telescope spectra. The amount of absorption is dependent upon the strength of the stellar wind. With guidance from hydrodynamic models of astrospheres, we use detected astrospheric Lyα absorption to estimate the stellar mass loss rates. For the solar-like GK stars in our sample, mass loss appears to increase with stellar activity, suggesting that young, active stars have stronger winds than old, inactive stars. However, Proxima Cen (M5.5 Ve) and λ And (G8 IV-III+M V) appear to be inconsistent with this relation.

1. Introduction

Until recently, the solar wind has been one solar phenomenon that has not been detectable around any other star. The massive winds of hot stars and evolved cool stars are detectable spectroscopically and have been studied for decades. But the wind we observe from the Sun is comparatively weak and fully ionized, making it impossible to directly detect similar winds around other cool main sequence stars like the Sun. The low mass loss rate of solar-like stars does not mean that their winds are unimportant. Winds are the primary mechanism by which cool stars shed angular momentum, resulting in an observed decrease in rotation rate as stars age, which in turn results in a decrease in stellar magnetic activity with time (i.e., starspot coverage, X-ray flux, flare rate, etc.). Also, the wind of the young Sun may have played a crucial role in the erosion of primordial planetary atmospheres (Ayres 1997).

[1]JILA, University of Colorado

[2]Institute of Geophysics and Planetary Physics, University of California at Riverside

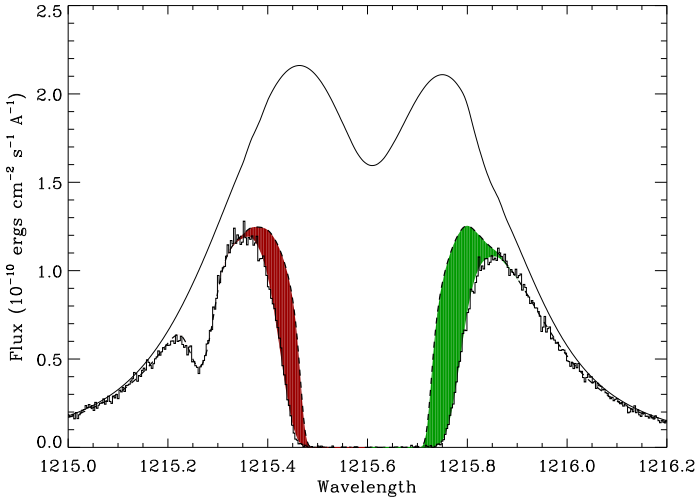

Figure 1. HST/GHRS observation of the Lyα line of α Cen B, showing broad H I absorption at 1215.6 Å and narrow D I absorption at 1215.25 Å. The assumed stellar line profile is shown as a solid line, and the dashed line shows the absorption from the ISM alone. The excess H I absorption seen in the data is due to heliospheric (green) and astrospheric (red) absorption.

Although solar-like winds cannot be detected directly, the UV spectrometers on the Hubble Space Telescope (HST), first GHRS and now STIS, provide a way to detect these winds indirectly, thanks to the Lyα absorption that is produced by the interaction region between the wind and surrounding ISM. Hydrodynamic models of the collision between the solar wind and the ISM predict that the collision should produce a population of heated H I throughout our heliosphere (Baranov & Malama 1995; Zank et al. 1996). This hot H I produces a broad Lyα absorption profile that in some cases is detectable in high resolution Lyα spectra of nearby stars, as long as the interstellar H I absorption is not too broad to obscure the heliospheric absorption (Linsky & Wood 1996; Gayley et al. 1997; Izmodenov, Lallement, & Malama 1999; Wood, Müller, & Zank 2000b). In some cases, "astrospheric" absorption around the observed star can also be detected on the blue side of the line rather than the red side where the heliospheric absorption resides (Wood, Alexander, & Linsky 1996; Dring et al. 1997; Wood & Linsky 1998).

2. The α Cen Example

Observations of our nearest stellar neighbors in the α Cen system (G2 V+K0 V) provided detections of both heliospheric and astrospheric H I absorption in the same spectrum. The Lyα profile of α Cen B (K0 V) is displayed in Figure 1, showing broad H I absorption and narrow deuterium (D I) absorption. When the interstellar H I absorption is constrained to have a central velocity and Doppler

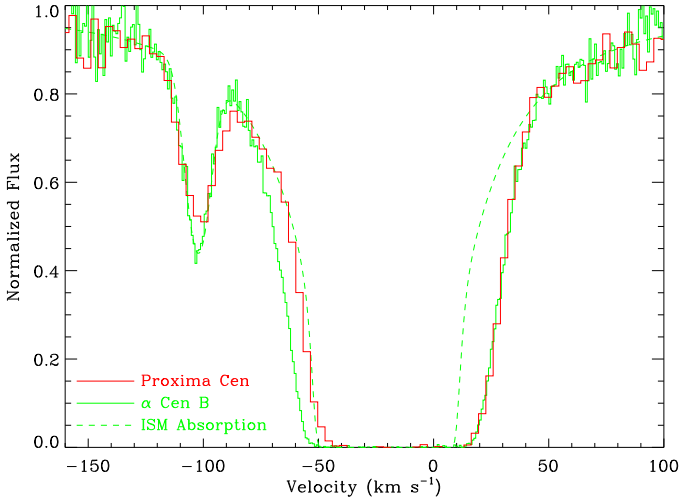

Figure 2. The HST/STIS α Cen B spectrum (green histogram) and inferred ISM absorption (green dashed line) are compared with a lower resolution STIS spectrum of α Cen's distant companion Proxima Cen (red histogram). The Alpha/Proxima Cen data agree well on the red side of the H I absorption where the heliospheric absorption lies, but on the blue side the Proxima Cen data do not show the excess Lyα absorption seen toward α Cen (i.e. the astrospheric absorption).

broadening parameter consistent with D I and other ISM lines, interstellar absorption cannot account for all of the observed H I absorption (Linsky & Wood 1996). Excess absorption exists on both sides of the interstellar H I line. Using hydrodynamic models of the heliosphere, Gayley et al. (1997) showed that heliospheric absorption could account for the red-side excess absorption but not the blue-side excess, which is best interpreted as astrospheric absorption. The models predict that heliospheric absorption will be redshifted relative to the ISM absorption regardless of the line of sight, primarily due to the deceleration of ISM material as it crosses the bow shock. Conversely, astrospheric absorption will generally always appear blueshifted from our perspective outside the stellar astrospheres.

Further proof that the blue side excess absorption toward α Cen is astrospheric is provided by observations of α Cen's distant companion Proxima Cen (M5.5 Ve). Figure 2 shows that the blue-side excess is *not* seen toward Proxima Cen, demonstrating that the blue-side excess toward α Cen A and B must indeed be due to circumstellar H I surrounding the α Cen binary that does not extend as far as Proxima Cen (Wood et al. 2001). The two α Cen stars show the same absorption because they are close enough to lie within the same astrosphere, unlike the distant ($\sim 12,000$ AU away) companion Proxima Cen.

3. Measuring Mass Loss Rates from Astrospheric Absorption

Larger mass loss rates yield larger astrospheres and thus more H I absorption, so the observed amount of astrospheric absorption can be used to estimate the mass loss rate. By computing a series of models of the α Cen astrosphere assuming different mass loss rates and using the models to predict astrospheric absorption, Wood et al. (2001) estimated the combined mass loss rate of α Cen A and B to be twice that of the Sun ($\dot{M} = 2\ \dot{M}_{\odot}$), noting that α Cen A and B are close enough for the winds of both stars to be contributing to the same astrosphere. An upper limit of 0.2 $\dot{M}_{\odot}$ was estimated for Proxima Cen.

Even before the blue-side excess absorption observed toward α Cen was clearly demonstrated to be astrospheric rather than heliospheric by Gayley et al. (1997), blue-side excess H I absorption was also detected toward ϵ Ind (K5 V) and λ And (G8 IV-III+M V), which was more easily attributed to astrospheric absorption since for these stars there is no evidence for any red-side excess that would indicate contamination from heliospheric absorption (Wood et al. 1996). Müller, Zank, & Wood (2001a) presented initial models of these two astrospheres. Based on these models and a few additional ones, the mass loss rates for ϵ Ind (K5 V) and λ And are estimated to be about 0.5 $\dot{M}_{\odot}$ and 5 $\dot{M}_{\odot}$, respectively (Müller, Zank, & Wood 2001b). Note that all the astrospheric models of α Cen, ϵ Ind, and λ And are extrapolated from a heliospheric model that succesfully reproduces the heliospheric absorption observed towards α Cen and other stars that show excess absorption on the red side of the H I Lyα line (Wood et al. 2000b).

Detections of astrospheric absorption have also been found for four other stars (ϵ Eri, 61 Cyg A, 40 Eri A, and 36 Oph; Dring et al. 1997; Wood & Linsky 1998; Wood, Linsky, & Zank 2000a), and mass loss measurements have been recently estimated for these stars (Wood et al., in preparation). For all stars with detected astrospheric absorption (except 40 Eri A), Figure 3 shows the comparison between the observed astrospheric absorption and that predicted by astrospheric models computed assuming different mass loss rates.

In principle, discrepancies between the models and the data can be lessened if changes are made to the stellar Lyα line profiles that have to be assumed in this analysis. However, it is difficult to shift the location where the H I absorption becomes saturated by any *reasonable* changes to the stellar profile. Thus, trying to correct discrepancies at the base of the absorption typically results in the introduction of unreasonable fine structure into the assumed stellar line profile (Wood et al. 2000b). The bottom line is that the base of the H I absorption is less affected by uncertainties in the stellar profile than the upper part of the H I absorption profile, so the base of the profile is the best place to compare the data and the models when deciding which model is the best fit. For this reason, we consider the best fit to the ϵ Ind data to be the 0.5 $\dot{M}_{\odot}$ model rather than the 0.8 $\dot{M}_{\odot}$ model (see Fig. 3).

Figure 4 shows H I density maps for the hydrodynamic models of the astrospheres that best fit the data in Figure 3. Figure 4 provides some sense for the size scale of these astrospheres (in AU). The dashed line in each panel indicates the direction from the star towards the Sun. The red area in each panel is a density enhancement between the bow shock and "astropause" (analogous

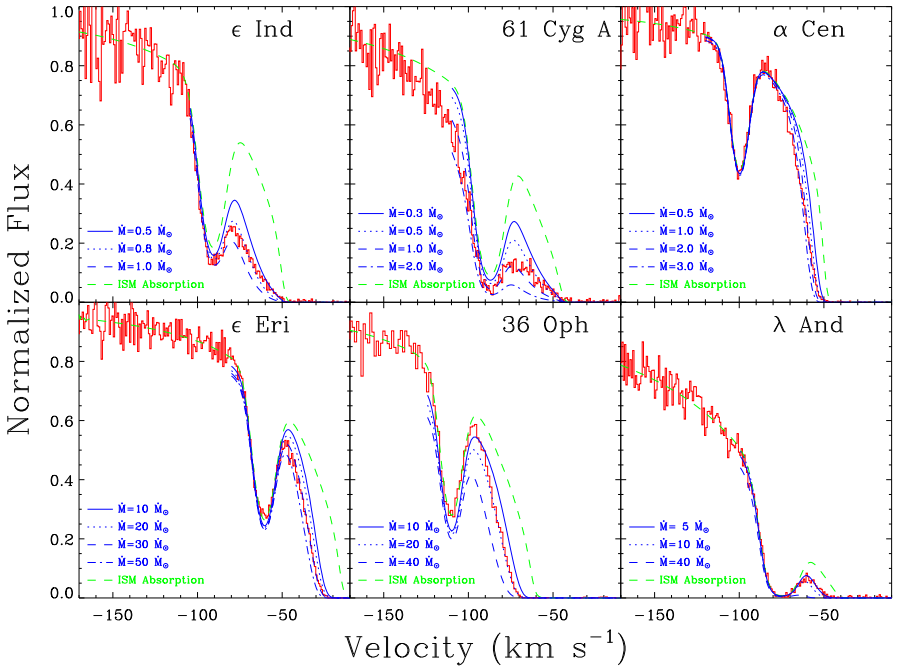

Figure 3. Closeups of the blue side of the H I Lyα absorption lines of all stars with detected astrospheric absorption, plotted on a heliocentric velocity scale. Narrow D I ISM absorption is visible in all the spectra just blueward of the saturated H I absorption. Green dashed lines indicate the interstellar absorption alone, and blue lines in each panel show the additional astrospheric absorption predicted by hydrodynamic models of the astrospheres assuming various mass loss rates.

to "heliopause") that has been called a "hydrogen wall" (Baranov & Malama 1995). The hydrogen wall is responsible for most of the astrospheric absorption that we are detecting in Figure 3.

All the mass loss measurements based on astrospheric analyses are listed in Table 1. This table also lists the interstellar wind velocity seen by the star, V_{ISM}, and the angle with respect to the upwind direction sampled by the Sun–star line of sight, θ (which is shown graphically in Fig. 4). These quantities, which must be known in order to model the astrospheres and predict astrospheric absorption, can be estimated from the known space motions of these nearby stars and the local ISM flow vector (Lallement et al. 1995). It is worth noting that the use of the local flow vector will only be an approximation for stars at the end of lines of sight that show more than one ISM velocity component. However, even when multiple components are observed in the local ISM, they are generally only separated by no more than 5–10 km s^{-1}, meaning the local cloud vector should still be a reasonable approximation.

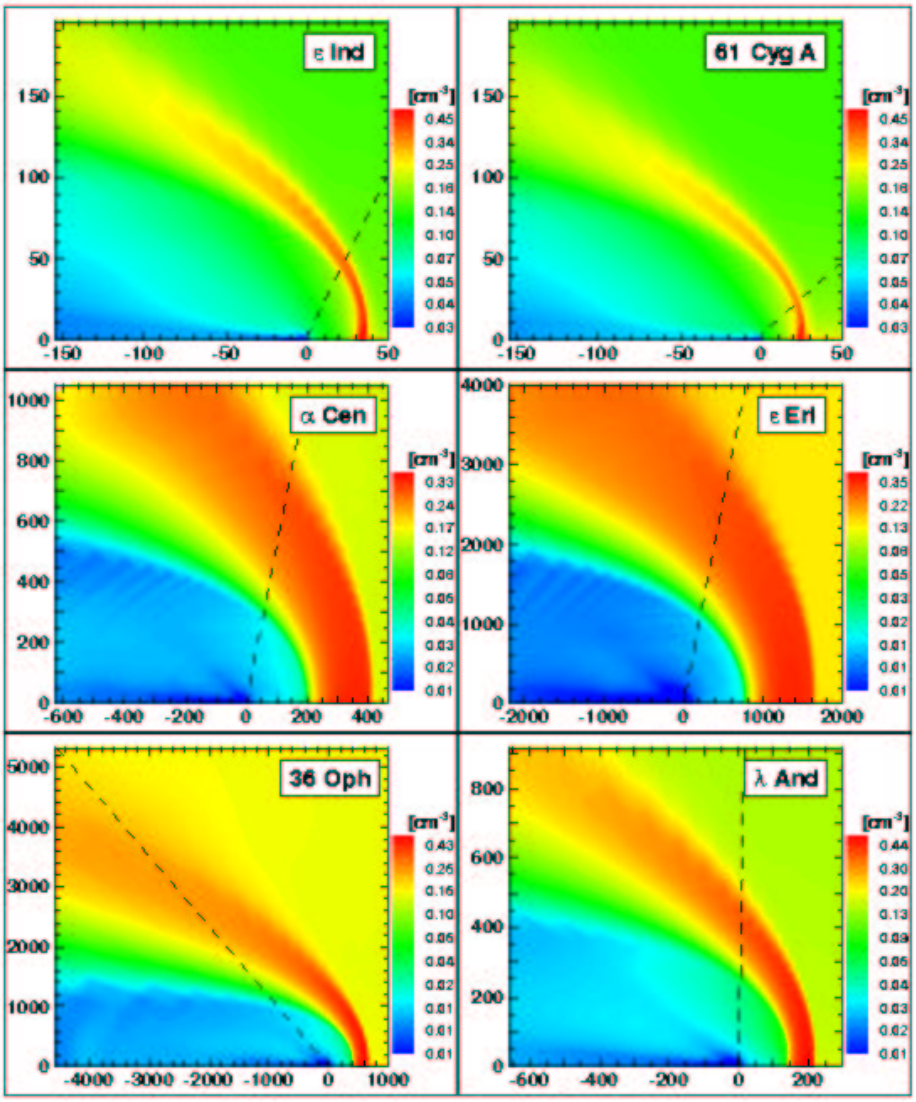

Figure 4. Maps of H I density from hydrodynamic models of stellar astrospheres. The models shown are the ones that lead to the best fits to the data in Fig. 3. The distance scale is in AU. The dashed lines indicate the Sun–star line of sight.

Two of the astrospheric detections listed in Table 1 have been flagged as being questionable detections. One of them, λ And, is questionable because there are no observations of narrow ISM lines such as Mg II h & k to provide information on the velocity structure of the ISM for that line of sight. As a consequence, the ISM absorption shown in Figure 3 for λ And is estimated assuming a single ISM absorption component. The single component analysis clearly suggests the existence of excess H I absorption on the blue side of the line that we are interpreting as being astrospheric (Wood et al. 1996), but the possibility exists that there is an additional ISM absorption component blueward of the main component which could conceivably account for the excess absorption without any need for an astrospheric contribution.

The 40 Eri A astrospheric absorption is questionable for an entirely different reason. The very fast ISM wind speed seen by this star (V_{ISM} = 127 km s^{-1}) yields an extremely broad and unsaturated astrospheric absorption profile, very different in appearance from those shown in Figure 3. As a consequence of this unsaturated profile, the detection of the astrospheric absorption is less secure (see Wood & Linsky 1998), and even if the detection is real such a profile makes it possible to alter the assumed stellar profile in ways that allow models assuming many different mass loss rates to be consistent with the data. As a consequence, we only list an upper limit for the mass loss rate for 40 Eri A ($\dot{M} < 5\ \dot{M}_{\odot}$), and even this result should be considered with some skepticism.

Table 1. Mass Loss Measurements

Star	Spectral Type	d (pc)	V_{ISM} (km s^{-1})	θ (deg)	$\dot{M}$ ($\dot{M}_{\odot}$)	Log L$_x$	Surf. Area (A$_{\odot}$)
α Cen	G2 V+K0 V	1.3	25	79	2	27.34	2.37
Prox Cen	M5.5 V	1.3	25	79	< 0.2	27.23	0.026
ϵ Eri	K1 V	3.2	27	76	30	28.32	0.62
61 Cyg A	K5 V	3.5	86	46	0.5	27.26	0.45
ϵ Ind	K5 V	3.6	68	64	0.5	27.18	0.50
40 Eri A[a]	K1 V	5.0	127	59	< 5	27.61	0.64
36 Oph	K1 V+K1 V	5.5	40	134	20	28.28	0.88
λ And[a]	G8 IV-III+M V	26	53	89	5	30.53	55

[a]Questionable detection.

4. Mass Loss as a Function of Activity

Since the winds of cool main sequence stars have their origins in the coronae of these stars, it is natural to wonder if mass loss rates are correlated with coronal properties. In Table 1, we list coronal X-ray luminosities for the stars with mass loss measurements. All the luminosities are based on ROSAT PSPC data. Most of the $\log L_X$ values are from Hünsch et al. (1999), with the exception of the λ And luminosity, which is from Ortolani et al. (1997). Following Schmitt, Fleming, & Giampapa (1995), we assume that 61 Cyg A contributes 64% of the binary's X-ray flux.

For an equitable comparison, it is necessary to normalize the mass loss measurements and X-ray luminosities by the stellar surface areas. We estimate stellar radii using the Barnes-Evans relation (Barnes, Evans, & Moffett 1978), except for Proxima Cen and λ And, for which we assume radii of 0.16 R$_{\odot}$ and

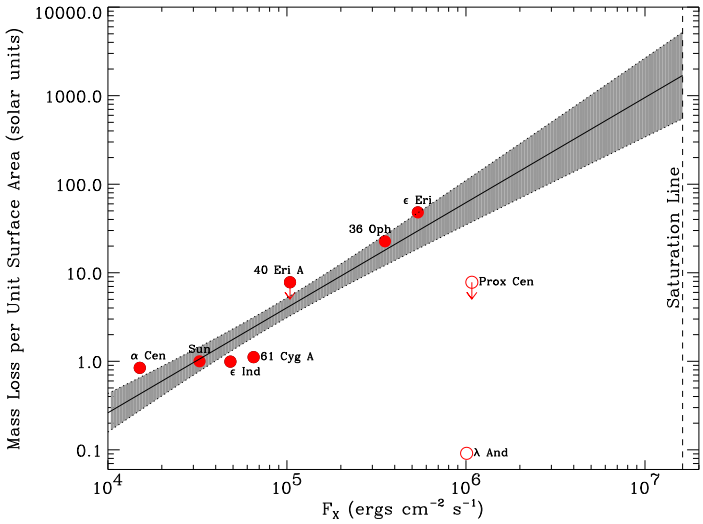

Figure 5. Measured mass loss rates (per unit surface area) plotted versus X-ray surface flux. A power law has been fitted to the solar-like GK dwarfs (filled circles), and the shaded region is the estimated uncertainty in the fit. Proxima Cen (M5.5 Ve) and λ And (G8 IV-III+M V) appear to be inconsistent with this relation. The saturation line represents the maximum F_X value observed for solar-like stars.

7.4 $R_\odot$, respectively (Panagi & Mathioudakis 1993; Nordgren et al. 1999). The last column of Table 1 lists the stellar surface areas derived from these radii (in solar units). Note that α Cen and 36 Oph are binary systems in which the two stars share the same astrospheres, and each member of the system is expected to be contributing to the combined stellar wind. Thus, for α Cen and 36 Oph the X-ray luminosity and surface area listed in Table 1 are the combined luminosity and area of both members of the binary.

Figure 5 shows mass loss rates per unit surface area plotted versus X-ray surface flux. For the solar-like GK dwarfs, the data suggest that more active stars have higher mass loss rates. The saturation line indicates the maximum X-ray flux observed from solar-like stars (Güdel, Guinan, & Skinner 1997). It is an interesting question why the M dwarf Proxima Cen and the RS CVn system λ And are inconsitent with the mass-loss/activity relation suggested by the solar-like stars. It had been proposed in the past that flares on active M dwarfs such as Proxima Cen should induce large mass loss rates (e.g., Mullan & Linsky 1999), but Figure 5 suggests that Proxima Cen has a significantly *lower* mass loss rate than the solar-like stars would predict. Explaining why M dwarf flare stars should have low mass loss rates promises to be a challenge for models of coronal mass loss. The λ And data point in Figure 5 is even more discrepant than Proxima Cen, but the uncertainty regarding the reality of the astrospheric absorption precludes any detailed consideration of its mass loss behavior at this time (see above).

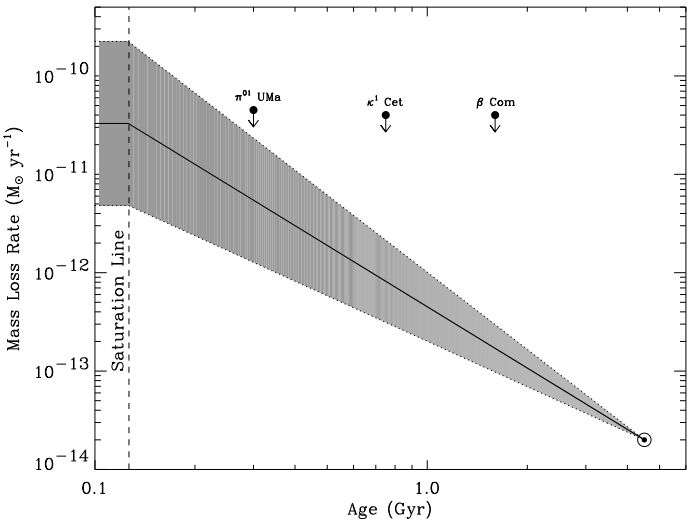

Figure 6. The mass loss history of the Sun suggested by the power law relation from Fig. 5. The upper limits are based on radio nondetections of three solar-like stars (Gaidos et al. 2000).

A power law has been fitted to the solar-like stars in Figure 5. We use a Monte Carlo technique to estimate the best fit and its uncertainty. We assume uncertainties in the mass loss measurements of a factor of 2, and we also assume an uncertainty in the X-ray flux of a factor of 2 to crudely take into account potential X-ray variability. We randomly vary the data points within these error bars and perform a power law fit for each trial. The line shown in Figure 5 is the average fit and the shaded region represents the 1 σ uncertainty in the fit. Quantitatively, the result is

$$\dot{M} \propto F_x^{1.19\pm0.20}. \tag{1}$$

As stars age, their rotation rates (V_{rot}) slow down due to magnetic braking. As rotation slows, less magnetic activity is generated by the stellar dynamo, so X-ray fluxes decrease. Quantitatively, Ayres (1997) estimates for solar-like stars:

$$V_{rot} \propto t^{-0.6\pm0.1} \tag{2}$$

and

$$F_x \propto V_{rot}^{2.9\pm0.3}. \tag{3}$$

Combining equations 1–3, we can obtain the following relation for mass loss and stellar age:

$$\dot{M} \propto t^{-2.07\pm0.53}. \tag{4}$$

Figure 6 shows what this relation implies for the mass loss history of the Sun. The upper limits in the figure are based on nondetections of radio emission from three solar-like stars (Gaidos, Güdel, & Blake 2000).

Figure 6 suggests that the solar wind could have been as much as 1000 times stronger in the distant past. Besides its obvious relevance for solar and

stellar astrophysics, this result also has profound implications for the evolution of planetary atmospheres in our solar system, which can be drastically affected by solar wind erosion. The loss of water from the Martian atmosphere and surface may be a particularly interesting example of this (Perez de Tejada 1992; Kass & Yung 1995; Lundin 2001).

Acknowledgments. Support for this work was provided by NASA grant NAG5-9041 to the University of Colorado.

References

Ayres, T. R. 1997, JGR, 102, 1641

Baranov, V. B., & Malama, Y. G. 1995, JGR, 100, 14755

Barnes, T. G., Evans, D. S., & Moffett, T. J. 1978, MNRAS, 183, 285

Dring, A. R., Linsky, J. L., Murthy, J., Henry, R. C., Moos, W., Vidal-Madjar, A., Audouze, J., & Landsman, W. 1997, ApJ, 488, 760

Gaidos, E. J., Güdel, M., & Blake, G. A. 2000, GRL, 27, 501

Gayley, K. G., Zank, G. P., Pauls, H. L., Frisch, P. C., & Welty, D. E. 1997, ApJ, 487, 259

Güdel, M., Guinan, E. F., & Skinner, S. L. 1997, ApJ, 483, 947

Hünsch, M., Schmitt, J. H. M. M., Sterzik, M. F., & Voges, W. 1999, A&AS, 135, 319

Izmodenov, V. V., Lallement, R., & Malama, Y. G. 1999, A&A, 342, L13

Kass, D. M., & Yung, Y. L. 1995, Science, 268, 697

Lallement, R., Ferlet, R., Lagrange, A. M., Lemoine, M., & Vidal-Madjar, A. 1995, A&A, 304, 461

Linsky, J. L., & Wood, B. E. 1996, ApJ, 463, 254

Lundin, R. 2001, Science, 291, 1909

Mullan, D. J., & Linsky, J. L. 1999, ApJ, 511, 502

Müller, H. -R., Zank, G. P., & Wood, B. E. 2001a, ApJ, 551, 495.

Müller, H. -R., Zank, G. P., & Wood, B. E. 2001b, in The Outer Heliosphere: The Next Frontiers, in press.

Nordgren, T. E., et al. 1999, AJ, 118, 3032

Ortolani, A., Maggio, A., Pallavicini, R., Sciortino, S., Drake, J. J., & Drake, S. A. 1997, A&A, 325, 664

Panagi, P. M., & Mathioudakis, M. 1993, A&AS, 100 343

Perez de Tejada, H. 1992, JGR, 97, 3159

Schmitt, J. H. M. M., Fleming, T. A., & Giampapa, M. S. 1995, ApJ, 450, 392

Wood, B. E., Alexander, W. R., & Linsky, J. L. 1996, ApJ, 470, 1157

Wood, B. E., & Linsky, J. L. 1998, ApJ, 492, 788

Wood, B. E., Linsky, J. L., Müller, H. -R., & Zank, G. P. 2001, ApJ, 547, L49

Wood, B. E., Linsky, J. L., & Zank, G. P. 2000a, ApJ, 537, 304

Wood, B. E., Müller, H. -R., & Zank, G. P. 2000b, ApJ, 542, 493

Zank, G. P., Pauls, H. L., Williams, L. L., & Hall, D. T. 1996, JGR, 101, 21639